

Compliant Motion Control for Robot Manipulators (Input-Output Approach)

H. Kazerooni
J. Balkovicius
J. Guo

Mechanical Engineering Department
University of Minnesota, Minneapolis

Abstract

The work presented here is a controller design methodology for robot manipulators based on the input-output functional relationships [26] in the dynamic behavior of the robot manipulator and environment. This controller guarantees: 1) the robot end-point follows an input command vector "closely" when the robot is not constrained by the environment, and 2) the contact force is a function of the same input command vector (used in the unconstrained environment) when the robot is constrained by the environment. The controller is capable of "handling" both types of constrained and unconstrained maneuverings, and is robust to bounded uncertainties in the robot dynamics. The controller does not need any hardware or software switch for the transition between unconstrained and constrained maneuvering. A set of experiments has been carried out in reference 14 and 15 to show how this unified approach can develop compliant motion in a constrained maneuvering.

Nomenclature

A	the closed-loop mapping from r to f
d, e	$n \times 1$ vector of the external force on the robot end-point and $n \times 1$ input trajectory vector
e_m, d_m	positive scalars
E	environment dynamics
f	$n \times 1$ vector of the contact force
f_{∞}, y_{∞}	the limiting value of the contact force and robot position for rigid environment
G	robot dynamics with positioning controller
H	compensator transfer function matrix
r	$n \times 1$ input-command vector
n	degrees of the freedom of the system $n < 6$
S	robot manipulator stiffness
T	positive scalar
V	the forward loop mapping from e to f
x	environment deflection
y	$n \times 1$ vector of the robot end-point position
x_0	$n \times 1$ vector of the environment position before contact
θ	$n \times 1$ vector of the joint angles of the robot
ϵ_e, ϵ_d	positive scalars
ω_0	frequency range of operation (bandwidth)
α_1, β_1	positive scalars

1. Introduction

In general, manipulation consists of two categories. In the first category, the manipulator end-point is free to move in all directions. In the second, the manipulator end-point interacts mechanically with the environment. Most assembly operations and manufacturing tasks require mechanical interactions with the environment or with the object being manipulated, along with "fast" motion in free and unconstrained space. Therefore, the object of this work is to develop a control system such that the robot will be capable of "handling" both types of maneuvers without any hardware and software switches. The hardware and software switches used in algorithms such as hybrid force/position control [20] develop unpleasant transient response in the transition period. In meeting the above objective, the goal is to develop a controller for the robot manipulator such that:

1) The robot end-point follows an input-command vector very "closely" when the robot is not constrained (a more rigorous definition for "closely" will follow).

2) The contact force is a function of the same input-command used in the unconstrained maneuvering when the robot is constrained by the environment.

Note that the above notation does not imply a force control technique [18,19,28,29,30,31]. We are looking for a controller that guarantees the tracking of the input-command vector when the robot is not constrained, as well as the relation of the contact-force vector with the same input-command vector when the robot encounters an unknown environment.

2. Motivation

The following scenario reveals the crucial need for compliance control in high-speed manufacturing operations. Consider an assembly operation by a human worker in which there are parts to be assembled on the table. Each time the worker decides to reach the table and pick up a part, she/he always encounters the table with a non-zero speed; in other words she/he hits the table while picking up the parts. The worker also assembles the parts with a non-zero speed; meaning the parts hit each other while they are assembled. The ability of the human hand to encounter the unknown and

unstructured environment with non-zero speed allows for a higher speed of operation. This ability in human beings flags the existence of a compliance control mechanism in biological systems. This mechanism guarantees the "stability" of contact forces in constrained maneuvering, in addition to high speed maneuvering in an unconstrained environment. With the existing state of technology, we do not have an integrated robotic assembly system that can encounter an unstructured environment as a human worker can. No existing robotic assembly system is faster than a human hand. The compliancy in the human hand allows the worker to encounter the environment with non-zero speed. The above example does not imply that we choose to imitate human factory-level physiological/psychological behavior as our model to develop an over-all control system for manufacturing tasks such as assembly and finishing processes. We stated this example to show that: 1) a reliable and optimum solution for simple manufacturing tasks such as assembly does not yet exist and 2) it is the existence of an efficient, fast compliance control system in human beings that allows for superior and faster performance. We believe compliance control is one of the key issues in the development of high-speed manufacturing operations for robot manipulators.

The control method explained here is general and applies to all industrial and research manipulators. We take the time-domain non-linear approach to arrive at the stability condition. The results of experiments in reference 15 confirm the frequency domain approach.

3. The Controller Design Objectives

The design objective is to provide a stabilizing dynamic compensator for the robot manipulator such that the following design specifications are satisfied.

I. The robot end-point follows an input-command vector, r , when the robot manipulator is free to move.

II. The contact force, f , is a function of the input command vector, r , when the robot is in contact with the environment.

The first design specification allows for free manipulation when the robot is not constrained. If the robot encounters the environment, then according to the second design specification, the contact force will be a function of the input command vector. Thus, the system will not have a large and uncontrollable contact force. Note that r is an input command vector that is used for both unconstrained and constrained maneuverings. The end-point of the robot will follow r when the robot is unconstrained, while the contact force will be a function of r (preferably a linear function for some bounded frequency range of r) when the robot is constrained.

4. Non-Linear Dynamic Model of the Robot with Positioning Controllers

In this section we develop a new approach to describe the dynamic behavior of a large class of industrial and research robot manipulators having positioning controllers. We plan to model the dynamic behavior of these manipulators by a general mathematical form. *The fact that most industrial manipulators have some kind of*

robust positioning controllers is the motivation behind our approach. Also, a number of methodologies exist for the development of the robust positioning controllers for direct and non-direct robot manipulators (23,24,27).

The end-point position of a robot manipulator that has a positioning controller is "approximately" equal to the input trajectory vector, e , if e is bounded in magnitude. The approximate equality of e and the actual end-point position (in absence of external force on the robot end-point) can be represented by mapping G in equation 1.

$$y = G(e) \quad (1)$$

$$\text{where: } \frac{\|y - e\|_p}{\|e\|_p} < \epsilon_e \quad \text{for } \|e\|_p < e_m \quad (2)$$

e : The n -dimensional ($n \leq 6$) input trajectory vector in a global cartesian coordinate frame.

y : The n -dimensional ($n \leq 6$) actual position vector of the robot end-point in a global cartesian coordinate frame.

The definition for $\|\cdot\|_p$ (P-norm) is given in Appendix A. Note that e is the input trajectory vector that a commercial robot manipulator accepts via its positioning controller. Because of limitation on the size of the actuator torque, one cannot track a "large" trajectory vector, e , with a small error, ϵ_e . Scalar e_m is defined to represent the confinement of the norm ("magnitude" in the multivariable sense) of e . Regardless of the structure of this positioning controller, relationships 1 and 2 can be justified. One can always find an e_m and ϵ_e experimentally (or analytically if possible) for a particular robot manipulator.

Robot manipulators with positioning controllers are not infinitely stiff in response to external forces (also called disturbances). Even though the positioning controllers of robots are usually designed to follow the trajectory commands (according to relationships 1 and 2) and reject disturbances, the robot end-point moves somewhat in response to imposed forces on the robot end-point. The motion of the robot end-point in response to imposed forces is caused by either structural compliance in the robot or the positioning controller compliance. The motion of the end-point of a robot under the imposed force at the end-point, d , in the absence of any input trajectory vector can be represented by mapping S in equation 3.

$$y = S(d) \quad (3)$$

$$\text{where: } \frac{\|y\|_p}{\|d\|_p} < \epsilon_d \quad \text{for } \|d\|_p < d_m \quad (4)$$

Where d is the n -dimensional vector of the external force that is imposed on the robot end-point. The general form of the non-linear dynamic equations of a robot manipulator with positioning controller can be given by two non-linear vector functions G and S in equation 5. Note that, although we have assumed d and e effect the robot in a non-linear fashion, equation 5 assumes that the motion of the robot end-point is a linear addition of both effects.

$$y = G(e) + S(d) \quad (5)$$

Figure 1 shows the nature of the mapping in equation 4. No assumption on the internal structures of $G(e)$ and $S(d)$ are made. We assume that $G(e)$ and $S(d)$ are stable, non-linear

operators in the L_p -space; in other words $G: L_p^n \rightarrow L_p^n$, $S: L_p^n \rightarrow L_p^n$ and also there exist constants $\alpha_1, \beta_1, \alpha_2$, and β_2 such that $\|G(e)\|_p < \alpha_1 \|e\|_p + \beta_1$ and $\|S(d)\|_p < \alpha_2 \|d\|_p + \beta_2$. (The definition of stability in L_p -sense is given in Appendix A)

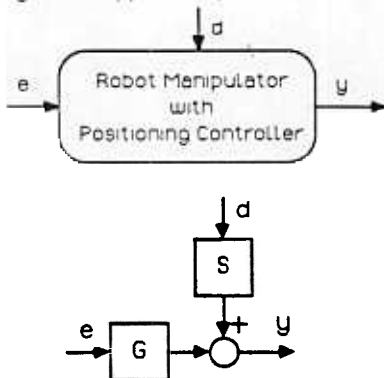


Figure 1: The Dynamic of the Manipulator with the Positioning Controller

5. Non-Linear Dynamic Behavior of the Environment

There is no specific model for the environment dynamics. The environment could be very "soft" or very "hard". We do not restrain ourselves to any geometry or to any structure. We can assume that if one point on the surface of the environment is displaced (e.g. by the end-point of the robot) as vector of x , then the required force to do such a task is defined by f (Figure 2).

The dynamic behavior of the environment is given by mapping E in equation 6. One can think of $E(x)$ as a $n \times 1$ vector function of x .

$$f = E(x) \quad (6)$$

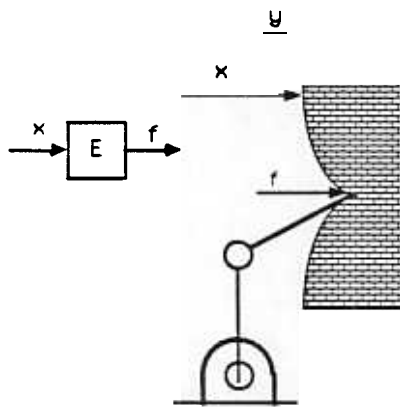


Figure 2: The Environment and Its Dynamics

x_0 is the the initial location of the point of contact before deformation occurs and y is the robot end-point position ($x = y - x_0$). No assumption is made on the structure of E . We also assume E is stable in L_p -sense; $E: L_p^n \rightarrow L_p^n$ and also there exist constants such as α_3 and β_3 such that $\|E(x)\|_p < \alpha_3 \|x\|_p + \beta_3$.

* In this paper force implies force and torque and position implies position and orientation.

6. Non-Linear Dynamic Behavior of the Robot Manipulator and Environment

Suppose a manipulator with dynamic equation 5 is in contact with an environment given by equation 6. The contact force will be equal to f . Note that when the robot manipulator and environment are in contact with each other, $f = -d$ and $x = y - x_0$. Figure 3 shows the robot manipulator and the environment when they are in contact with each other. Note that in some applications, the robot will have only uni-directional force on the environment. For example, in the grinding of a surface by a robot, the robot can only push the surface. If we consider positive f_i for "pushing" and negative f_i for "pulling", then in this class of manipulation, the robot manipulator and the environment are in contact with each other only along those directions where $f_i > 0$ for $i = 1, \dots, n$. In some applications such as screwing a bolt, the interaction force can be positive and negative. This means the robot can have clockwise and counter-clockwise interaction torque. The non-linear discriminator block-diagram in Figure 3 is drawn with dashed-line to illustrate the above concept. Considering equations 5 and 6, equations 7 and 8 represent the entire dynamic behavior of the robot and environment as a whole.

$$y = G(e) - S(f) \quad (7)$$

$$f = E(x)$$

$$\text{where } x = y - x_0 \quad (8)$$

The block diagram in Figure 3 shows the nature of mappings 7 and 8.

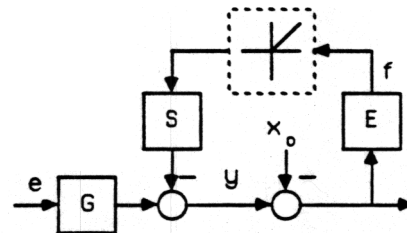


Figure 3: Interaction of the Robot Manipulator with the Environment

When the robot is not in contact with the environment, then $x = 0$ and the equation that governs the dynamics of the system is given by equation 1 ($y = G(e)$). Note the natural feedback in the system; the force developed in the system from the interaction of the robot manipulator and the environment affects the robot motion in a feedback fashion. We define V in equation 9 as a mapping from e to f in Figure 3.

$$f = V(e) \quad (9)$$

In other words the mappings given by equations 7 and 8 can be simplified by mapping $V: e \rightarrow f$ where e and f are shown in Figure 4. Note that we assume V is a stable operator in L_p -sense; in other words: $V: L_p^n \rightarrow L_p^n$ and also $\|V(e)\|_p < \alpha_4 \|e\|_p + \beta_4$ where α_4 and β_4 are constants.

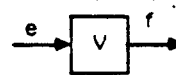


Figure 4: The Mapping from the Trajectory to the Contact Force

7. The Closed-Loop Architecture of the Closed-Loop System

The control architecture in Figure 5 shows how we

robot manipulators have linear dynamic behavior, it is more reasonable to use frequency domain techniques for controller design. This frequency domain technique also gives more insights to the problem. In the following sections, we use frequency domain to represent the dynamic behavior of the robot manipulator with positioning controller and the environment. Having the dynamic interaction of the robot manipulator and environment modeled in frequency domain, we consider the stability analysis of the closed-loop system shown in Figure 5. Using the Multivariable Nyquist Criteria, we will arrive at the sufficient condition on H that leads to stability of the closed-loop system shown in Figure 5. This condition on H confirms the results of Section 8.

9. Dynamic Behavior of the Robot Manipulator with Positioning Controller in Frequency Domain.

We define a transfer function matrix, G in equation 21 to define the dynamic behavior of a robot manipulator with positioning controller. Readers can think of G as a describing function matrix that maps the amplitude of the input trajectory, e , to the amplitude of the robot position, y . Since the dynamic behavior of robot manipulators with positioning controllers is generally considered non-linear, the output position amplitude, y , depends not only on the amplitude of the input trajectory, e , but also on the orientation of the robot, θ . For a given θ as the operating point.

$$y(j\omega, \theta) = G(j\omega, \theta) e(j\omega) \quad (21)$$

where:

$$\frac{\| (G(j\omega, \theta) - I_n) e(j\omega) \|_2}{\| e(j\omega) \|_2} < \epsilon_e \quad \text{for all } \omega \in \omega_o, \| \theta \|_2 < \epsilon_m \quad (22)$$

Some explanations are needed for the practical conditions that are imposed by ϵ_m and ω_o on inequality 22. Because of the limitation on the size of the actuator torque, one cannot track a "large" input trajectory, e , with a small tracking error, ϵ_e , within the frequency range of $[0, \omega_o]$. Scalar ϵ_m is defined to represent the confinement of the magnitude of e . Physical systems are not responsive to high frequency input trajectory commands. Inequality 22 will not hold at high frequencies. ω_o is introduced to represent this limitation. The frequency range $[0, \omega_o]$ where inequality 22 holds, is called the bandwidth of the closed-loop positioning system (1,5,9). ϵ_e is a small number for good positioning systems. As an example, for the ADEPT robot, ϵ is equal to 0.01 for all $\| \theta \|_2 < 1$ cm, and $\omega \in [0, 5$ hertz).

Note that we chose the frequency domain to represent the dynamic behavior of the closed-loop positioning robot. This allows us to represent an approximation of the dynamic behavior of the closed-loop positioning robot without being specific about the nature of the input trajectory, e , and the structure of the positioning controller. For any manipulator, with any type of positioning controller, one can always arrive at inequality 22 experimentally or analytically. Conservative values for ω_o and ϵ_m are adequate to represent an approximation of the closed-loop positioning dynamic for the robot.

We express the dynamic behavior of a robot manipulator in response to forces on the robot end-point similarly. We can express the stiffness of a robot manipulator by a matrix, S . The motion of the end-point of

a robot under the imposed force, d , at the end-point, in the absence of any input trajectory vector can be given by equation 23.

$$y(j\omega, \theta) = S(j\omega, \theta) d(j\omega) \quad (23)$$

$$\frac{\| S(j\omega, \theta) d(j\omega) \|_2}{\| d(j\omega) \|_2} < \epsilon_e \quad \text{for all } \omega \in \omega_o, \| \theta \|_2 < \epsilon_m \quad (24)$$

S is a transfer function matrix that represents the compliance (1/stiffness) of the robot. S is called the sensitivity matrix and for "good" positioning systems is quite "small". [By "small" we mean the maximum singular value of S is a small number for all the frequencies that the external force, d affects the system.]

Combining equations 21 and 23 into equation 25, one can represent the dynamic behavior of a robot with a positioning controller:

$$y(j\omega, \theta) = G(j\omega, \theta) e(j\omega) + S(j\omega, \theta) d(j\omega) \quad (25)$$

where G and S are given by equations 21 and 23. Figure 1 shows the complete dynamic behavior of the robot manipulator with a positioning controller.

11. Dynamic Behavior of the Environment in Frequency Domain

As we described in Section 5, we do not consider any specific model for the dynamic behavior of the environment. The environment dynamic behavior varies significantly for various robotic applications. We assume that if one point on the surface of environment is displaced (e.g. by the end-point of the robot) as vector of x , then the required force to do such a task is defined by

$$f(j\omega) = E(j\omega) x(j\omega) \quad (26)$$

$E(j\omega)$ is a complex matrix that maps the amplitude of the displacement vector, x to the amplitude of the contact force, f . The matrix E is a $n \times n$ matrix transfer function. No assumption about E is made; E is a singular matrix when the robot interacts with the environment in some directions only. For example, in grinding a surface, the robot is constrained by the environment in the direction normal to the surface only. Readers can be convinced of the truth of equation 26 by analyzing the relationship of the force and displacement of a spring as a simple model of the environment. E resembles the stiffness of a spring.

12. Dynamic Behavior of the Robot Manipulator and Environment in Frequency Domain

If a manipulator with dynamic equation 25 is in contact with an environment given by equation 26, then $f = -d$ and $x = y - x_o$. Combining equations 25 and 26, equation 27 is derived to describe the dynamic behavior of the robot and the environment. (For simplicity in notation, the arguments of functions are omitted.)

$$y = [I + SE]^{-1} G e \quad (27)$$

Figure 3 shows the robot manipulator and the environment when they are in contact with each other. When the robot is not in contact with the environment, then $x=0$ and the equation that governs the dynamics of the system is given by equation 28 (the same as equation 21).

$$y = G e \quad (28)$$

13. The Architecture of the Closed-Loop System

The control architecture in Figure 5 shows how

compliance is developed in the system. $H(j\omega)$ is a compensator to be designed. The input to this compensator is the contact force. The compensator output signal is being subtracted from the input command vector, r , resulting in the error signal, e as the trajectory command for the robot manipulator.

When the robot and the environment are in contact, then the value of the contact force and the end-point position of robot are given by equations 29 and 30 respectively.

$$f = E(1 + SE + GHE)^{-1} Gr \quad (29)$$

$$y = (1 + SE + GHE)^{-1} Gr \quad (30)$$

It is desired to choose a class of transfer function matrices, H , as compensators to control the contact force with input command r . When the system is not in contact with the environment, the actual position of the robot end-point can be commanded by the input trajectory command via the robot positioning controller. When the system is in contact with the environment, then the contact force follows r according to equation 29. In our approach, the input command vector, r , is used differently for the two categories of maneuverings. r is used as an input trajectory command in unconstrained space (in 28 $r=e$) and as a command to control force in constrained space, (equation 29). This method can be called Impedance Control (2,3,4,5,6) because it accepts a position vector as input and it reflects a force vector as output. We do not command any set-point for force as we do in force control systems (20,28). There is no hardware or software switch in the control system when the robot travels from unconstrained space to constrained space. The feedback loop on the contact force closes naturally when the robot encounters the environment.

14. Very Rigid Surface

In most manufacturing tasks such as robotic deburring, the end-point of the robot manipulator is in contact with a very stiff environment (8,12,13,14,15) In this section, we plan to calculate the limiting value for f and y when the robot manipulator and a very rigid environment are interacting with one another. According to the results in Appendix B, when the environment is very stiff, E is very "large" in the singular value sense, the resulting value for the contact force and the end-point position are given by equations 31 and 32 respectively:

$$f_{\infty} = (S+GH)^{-1} Gr \quad (31)$$

$$y_{\infty} = 0 \quad (32)$$

Since $G \approx I_n$ for all $\omega \in (0, \omega_0)$, the value of the contact force, f , within the bandwidth of the system $(0, \omega_0)$ can be approximated by equation 33:

$$f_{\infty} \approx (S+H)^{-1} r \quad \text{for all } \omega \in (0, \omega_0) \quad (33)$$

By knowing S and choosing H , one can shape the contact force. If H is chosen such that $(S+H)$ is "large" in the Singular Value sense* at high frequencies, then the contact force in response to high frequency components of r will be small. The value of $(S+H)$ within $(0, \omega_0)$ is the designer's choice and, depending on the task, it can have

* The maximum singular value of H is defined as:

$$\sigma_{\max}(H) = \max \frac{\|Hr\|_2}{\|r\|_2}$$

where $r \neq 0$, and $\|\cdot\|_2$ denotes the Euclidean norm

various values in different directions (6,7,10,11,22). A large value for $(S+H)$ within $(0, \omega_0)$ develops a compliant system while a small $(S+H)$ generates a stiff system.

15. Stability

The objective of this section is to arrive at a sufficient condition for stability of the system shown in Figure 5. This sufficient condition automatically leads to the introduction of a class of compensators, H , that can be used to develop compliance for the class of robot manipulators that have positioning controllers. The detailed derivation for the stability condition is given in Appendix C. According to the results of Appendix C, the sufficient condition for stability is given by inequality 34.

$$\sigma_{\max}[GHE] \leq \sigma_{\min}[SE + I_n] \quad \text{for all } \omega \in (0, \infty) \quad (34)$$

or,

$$\sigma_{\max}[H] \leq \frac{1}{\sigma_{\max}[E(SE + I_n)^{-1}G]} \quad \text{for all } \omega \in (0, \infty) \quad (35)$$

If H is chosen outside of this class, instability and consequent separation may occur. Inequality 35 is a sufficient condition for stability. If inequality 35 is not satisfied, no conclusion on the stability of the system can be achieved. $E(SE + I_n)^{-1}G$ is the forward loop transfer function of the system in Figure 7. According to inequality 35, the "size" of H in all directions must be smaller than the reciprocal of the maximum "size" of the forward loop transfer function, $E(SE + I_n)^{-1}G$. Inequality 35 guarantees the stability of the system if the maximum singular value of H is chosen to be less than the reciprocal of the maximum singular value of $E(SE + I_n)^{-1}G$.

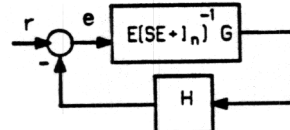


Figure 7: The Simplified Form of the System in Figure 5

Inequality 35 reveals some facts about the size of H . The smaller the sensitivity of the robot manipulator is, the smaller H must be chosen. Also from inequality 35, the more rigid the environment is, the smaller H must be chosen. In the "ideal case", no H can be found to allow a perfect positioning system ($S=0$) to interact with an infinitely rigid environment ($E=\infty$).

Stability for very rigid environment. If H is chosen to guarantee the compliance in the system according to equation 33, then it must also satisfy the stability condition. It can be shown that the stability criteria for interaction with a very rigid environment is given by inequality 36:

$$\sigma_{\max}[H] \leq \frac{1}{\sigma_{\max}[S^{-1}G]} \quad \text{for all } \omega \in (0, \infty) \quad (36)$$

It is clear that if the environment is very rigid, then one must choose a very small H to satisfy the stability of the system when S is "small". (A good positioning system has "small" S). Since $G \approx I_n$ for all $\omega \in (0, \omega_0)$, the bound for H ,

for a rigid environment and a "small" stiffness, is given by inequality 37.

$$\sigma_{\max} [H] \leq \sigma_{\min} [S] \quad \text{for all } \omega \in (0, \omega_0) \quad (37)$$

Stability Condition when $n=1$. In the case of the one degree of freedom system in Figure 8 the condition for stability is given by inequality 38.

$$\|HG\|_2 < \|(S+1/E)\|_2 \quad \text{for all } \omega \in (0, \infty) \quad (38)$$

Since in many cases $G \approx 1$ for all $0 < \omega < \omega_0$, then H must be chosen such that the following inequality is satisfied.

$$\|H\|_2 < \|(S+1/E)\|_2 \quad \text{for all } \omega \in (0, \omega_0) \quad (39)$$

Inequality 39 clearly shows that the more rigid the environment is, the smaller H must be chosen to guarantee the stability of the closed-loop system. In the case of a rigid environment ("large" E) and a "good" positioning system, H must be chosen as a very small gain.

16. Summary and Conclusion

Manipulation requires interaction with the environment or with the object being manipulated. This paper presents a controller architecture for the robot manipulators that can generate electronic compliancy. We started with modeling the class of robot manipulators that have positioning controllers. This model is independent of the structure of the positioning controller of the robot manipulator. Having the robot and environment modeled in a very general form, we arrive at a new architecture control to guarantee electronic compliancy for the robot manipulators. This approach allows not only for tracking the input-command vector, but also for compliancy in the system. The bound for the global stability of the manipulator and environment has been derived.

Appendix A

Definitions 1 to 5 will be used in proof of the stability of the closed-loop system (25,26).

Definition 1: For all $p \in (1, \infty)$, we label as L_p^n the set consisting of all functions $f = [f_1, f_2, \dots, f_n]^T: (0, \infty) \rightarrow \mathbb{R}^n$ such that:

$$\int_0^\infty \|f_i\|^p dt < \infty$$

Definition 2: For all $T \in (0, \infty)$, the function f_T defined by:

$$f_T = \begin{cases} f & 0 \leq t \leq T \\ 0 & T < t \end{cases}$$

is called the truncation of f to the interval (0, T).

Definition 3: The set of all functions $f = [f_1, f_2, \dots, f_n]^T: (0, \infty) \rightarrow \mathbb{R}^n$ such that $f_T \in L_p^n$ for all T is denoted by L_p^n although f by itself may or may not belong to L_p^n .

Definition 4: The norm on L_p^n is defined by:

$$\|f(\cdot)\|_p = \left(\sum_{i=1}^n \|f_i(\cdot)\|_p^2 \right)^{1/2}$$

Definition 5: Let $V(e): L_p^n \rightarrow L_p^n$. We say the mapping V is L_p -stable operator, if:

a) $V(e): L_p^n \rightarrow L_p^n$

b) $\|V(e)\|_p < \alpha_4 \|e\|_p + \beta_4$, where α_4 and β_4 are positive constants. According to this definition first we assume the

function maps from L_p^n to L_p^n . It is very clear that if one does not show that $V: L_p^n \rightarrow L_p^n$, therefore the satisfaction of condition (a) is impossible because L_p^n contains L_p^n . Once the mapping from L_p^n to L_p^n is established, then we say that the system is L_p -stable if, whenever the input belongs to L_p^n , the resulting output belong to L_p^n and moreover the norm of the output is no larger than than α_4 times the norm of the input plus the constant β_4 .

Proof of the stability theorem

Define the closed-loop mapping $A: r \rightarrow e$ (Figure 6).

$$e = r - HV(e) \quad (A1)$$

For each finite T, inequality A2 is true.

$$\|e\|_{p_e} < \|r\|_{p_e} + \|HV(e)\|_{p_e} \quad \text{for all } t \in (0, T) \quad (A2)$$

Since $HV(e)$ is L_p -stable. Therefore, inequality A3 is true.

$$\|e\|_{p_e} < \|r\|_{p_e} + \alpha_5 \|e\|_{p_e} + \beta_5 \quad \text{for all } t \in (0, T) \quad (A3)$$

$$\|e\|_{p_e} < \frac{\|r\|_{p_e}}{1-\alpha_5} + \frac{\beta_5}{1-\alpha_5} \quad \text{for all } t \in (0, T) \quad (A4)$$

Inequality A4, shows that $e(\cdot)$ is bounded over (0, T). Because this reasoning is valid for every finite T, it follows that $e(\cdot) \in L_p^n$, i.e., that $A: L_p^n \rightarrow L_p^n$. Next we show that the mapping A is L_p -stable in the sense of definition 5. Since $r \in L_p^n$, therefore $\|r\|_p < \infty$ for all $t \in (0, \infty)$, therefore inequality A5 is true.

$$\|e\|_p < \infty \quad \text{for all } t \in (0, \infty) \quad (A5)$$

Inequality A5 implies e belongs to L_p -space whenever r belong to L_p -space. With the same reasoning from equations A1 to A5, it can be shown that inequality A6 is true.

$$\|e\|_p < \frac{\|r\|_p}{1-\alpha_5} + \frac{\beta_5}{1-\alpha_5} \quad (A6)$$

Inequality A6 and A5 taken together, guarantee that the closed-loop mapping A is L_p -stable.

Appendix B

A very rigid environment generates a very large force for a small displacement. We choose the maximum singular value of E to represent the size of E. The following theorem states the limiting value of the force when the robot manipulator is in contact with a very rigid environment.

Theorem

If $\sigma_{\min}(E) > M$, where M is an arbitrarily large number, then the value of the force given by equation 10 will approach the expression given by equation B1

$$f_\infty = (S+GH)^{-1} G r \quad (B1)$$

Proof:

We will prove that $\|f_\infty - f\|_2$ approaches a small number as M approaches a large number.

$$f_\infty - f = (S+GH)^{-1} [I_n - (S+GH)^{-1} E (I_n + SE + GHE)^{-1}] G r \quad (B2)$$

Factoring $(I_n + SE + GHE)^{-1}$ to the right hand side:

$$f_\infty - f = (S+GH)^{-1} [I_n + SE + GHE]^{-1} G r \quad (B3)$$

$$\|f_\infty - f\|_2 < \sigma_{\max} [S+GH]^{-1} \sigma_{\max} [I_n + SE + GHE]^{-1} \sigma_{\max} [G] \|r\|_2 \quad (B4)$$

$$\|f_\infty - f\|_2 < \frac{\sigma_{\max} [G] \|r\|_2}{\sigma_{\min} [S+GH] (\sigma_{\min} [SE + GHE] - 1)} \quad (B5)$$

$$\|f_\infty - f\|_2 < \frac{\sigma_{\max} [G] \|r\|_2}{\sigma_{\min} [S+GH] (\sigma_{\min} [S+GH] \sigma_{\min} [E] - 1)} \quad (B6)$$

$\sigma_{\max}(G)$ and $\sigma_{\min}(S+GH)$ are bounded values. If $\sigma_{\min}(E) > M$, then it is clear that the left hand side of inequality B6 can be arbitrarily small number by choosing M to be a large number. The proof for $y_{\infty} = 0$ is similar to the above.

Appendix C

The objective is to find a sufficient condition for stability of the closed-loop system in Figure 5 by Nyquist Criteria. The block diagram in Figure 6 can be reduced to the block diagram in Figure A1 providing G^{-1} exists.

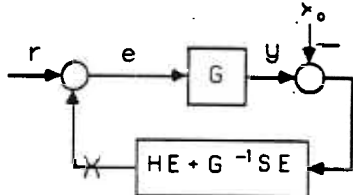


Figure C1: Simplified Block-Diagram of the System in Figure 5

There are two elements in the feedback loop; HE and $G^{-1}SE$. $G^{-1}SE$ shows the natural force feedback while HE represents the controlled force feedback in the system. If $H=0$, then the system in Figure C1 reduces to the system in Figure 3 (a stable positioning robot manipulator which is in contact with the environment E.) The objective is to use Nyquist Criteria (17, 21) to arrive at the sufficient condition for stability of the closed system when $H=0$. The following conditions are regarded:

- 1) The closed loop system in Figure A1 is stable if $H=0$. This condition simply states the stability of the robot manipulator and environment when they are in contact. (Figure 3 shows this configuration.)
- 2) H is chosen as a stable linear transfer function matrix. Therefore the augmented loop transfer function $\{GHE+SE\}$ has the same number of unstable poles that SE has. Note that in many cases SE is a stable system.
- 3) Number of poles on $j\omega$ axis for both loop SE and $G(HE+G^{-1}SE)$ are equal.

Considering that the system in Figure A1 is stable when $H=0$, we plan to find how robust the system is when the term HE is added to the feedback loop. If the loop transfer function $G(G^{-1}SE)$ (without compensator, H) develops a stable closed-loop system, then we are looking for a condition on H such that the augmented loop transfer function $G(HE+G^{-1}SE)$ guarantees the stability of the closed-loop system. According to the Nyquist Criteria, the system in Figure C1 remains stable if the clockwise encirclement of the $\det.[SE+GHE+I_n]$ around the center of the S-plane is equal to the number of unstable poles of the loop transfer function $[SE+GHE]$. According to conditions 2 and 3, the loop transfer functions SE and $[SE+GHE]$ both have the same number of unstable poles. The closed-loop system when $H=0$ is stable according to condition 1; the encirclements of $\det.[SE+I_n]$ is equal to unstable poles of SE. When H is added to the system, for stability of the closed-loop system, the number of the encirclements of $\det.[SE+GHE+I_n]$ must be equal to the number of unstable poles of the $[SE+GHE]$. Since the number of unstable poles of $[SE+GHE]$ and SE are the same, therefore for stability of the system $\det.[SE+GHE+I_n]$ must have the same number of encirclements that $\det.[SE+I_n]$

has. To guarantee the equality of the number of encirclements of $\det.[SE+GHE+I_n]$ and $\det.[SE+I_n]$, therefore $\det.[SE+GHE+I_n]$ must not pass through the origin of the s-plane or equivalently:

$$\det.[SE+GHE+I_n] \neq 0 \quad \text{for all } \omega \in [0, \infty) \quad (C1)$$

A sufficient condition to guarantee that $\det.[SE+GHE+I_n]$ is not equal to zero is given by inequality C2.

$$\text{or } \sigma_{\max}[GHE] < \sigma_{\min}(SE+I_n) \quad \text{for all } \omega \in [0, \infty) \quad (C2)$$

$$\sigma_{\max}[H] < \frac{1}{\sigma_{\max}(E(SE+I_n)^{-1}G)} \quad \text{for all } \omega \in [0, \infty) \quad (C3)$$

Note that $E(SE+I_n)^{-1}G$ is the transfer function matrix that maps e to the contact force, f. Figure 7 shows the closed-loop system. According to the result of the theorem, H must be chosen such that the size of H is smaller than the reciprocal of the size of the forward loop transfer function, $E(SE+I_n)^{-1}G$.

References

- 1) Doyle, J. C., Stein, G., "Multivariable Feedback Design: Concepts for a Classical / Modern Synthesis", IEEE Transaction on Automatic Control AC-26(1):1-16, February, 1981.
- 2) Hogan, N., "Adaptive Control of Mechanical Impedance by Coactivation of Antagonistic Muscles", IEEE Transaction on Automatic Control AC-29(7), July, 1984.
- 3) Hogan, N. "Impedance Control of Industrial Robots", Journal of Robotics and Computer Integrated Manufacturing 1(1):97-113, 1984.
- 4) Hogan, N., "Impedance Control: An Approach to Manipulation, Part 1: Theory, Part 2: Implementation, Part 3: Applications", ASME Journal of Dynamic Systems, Measurement, and Control, 1985.
- 5) Kazerooni, H., Houpt, P. K., "On The Loop Transfer Recovery", International Journal of Control, Volume, 43, Number 3, March 1986.
- 6) Kazerooni, H., Houpt, P. K., Sheridan, T. B., "Fundamentals of Robust Compliant Motion for Manipulators", IEEE Journal of Robotics and Automatic, N2, V2, June 1986
- 7) Kazerooni, H., Houpt, P. K., Sheridan, T. B., "A Design Method for Robust Compliant Motion of Manipulators", IEEE Journal of Robotics and Automation, N2, V2, June 1986.
- 8) Kazerooni, H., Bausch, J. J., Kramer, B., "An Approach to Automated Deburring by Robot Manipulators", ASME Journal of Dynamic Systems, Measurements and Control, December 1986.
- 9) Kazerooni, H., Houpt, P. K., Sheridan, T. B., "An Approach to Loop Transfer Recovery using Eigenstructure Assignment". In proceedings of the American Control Conference, June 1985, Boston.
- 10) Kazerooni, H., Houpt, P. K., Sheridan, T. B., "Robust Compliant Motion for Manipulators", In proceeding of the International Conference on Robotics and Automation, San Francisco, April 1986.
- 11) Kazerooni, H., Houpt, P. K., Sheridan, T. B., "Robust Design Method For Impedance control of Robot Manipulators", In proceeding of the American Control Conference, Seattle, June 1986.
- 12) Kazerooni, H., Bausch, J. J., Kramer, B., "An approach to Robotic Deburring". In proceeding of American

- Control Conference , Seattle, June 1986.
- 13) Kazerooni, H., "Automated Robotic Deburring Using Electronic Compliancy; Impedance Control", In proceedings of the IEEE International Conference on Robotics and Automation, Raleigh, North Carolina, March 1987.
 - 14) Kazerooni, H., Guo, J., "Design and Construction of an Active End-Effector", IEEE In proceedings of the IEEE International Conference on Robotics and Automation, Raleigh, North Carolina, March 1987.
 - 15) Kazerooni, H., " Robust Non-linear Impedance Control for Robot Manipulators", IEEE In proceedings of the IEEE International Conference on Robotics and Automation, Raleigh, North Carolina, March 1987.
 - 16) Lancaster, P., *Lambda-Matrices and Vibrating Systems*. Pergamon Press, 1966.
 - 17) Lehtomaki, N. A., Sandell, N. R., Athans, M., "Robustness Results in Linear-Quadratic Gaussian Based Multivariable Control Designs", IEEE Transaction on Automatic Control AC-26(1):75-92, February, 1981.
 - 18) Mason, M. T., "Compliance and Force Control for Computer Controlled Manipulators", IEEE Transaction on Systems, Man, and Cybernetics SMC-11(6):418-432, June, 1981.
 - 19) Paul, R. P. C., Shimano, B., "Compliance and Control", In Proceedings of the Joint Automatic Control Conference, pages 694-699. San Francisco, 1976.
 - 20) Raibert, M. H., Craig, J. J., "Hybrid Position/Force Control of Manipulators", ASME Journal of Dynamic Systems, Measurement, and Control 102:126-133, June, 1981.
 - 21) Safonov, M. G., Athans, M., Gain and Phase Margin for Multiloop LQG Regulators", IEEE Transaction on Automatic Control AC-22(2):173-179, April, 1977.
 - 22) Salisbury, K. J., "Active Stiffness Control of Manipulator in Cartesian Coordinates", In Proceedings of the 19th IEEE Conference on Decision and Control, pages 95-100. IEEE, Albuquerque, New Mexico, December, 1980.
 - 23) Slotine, J. J. , "Sliding Controller Design for Non-linear Systems", International Journal of Control, 1984, V40, N2.
 - 24) Slotine, J. J., "The robust Control of of Robot Manipulators", The international Journal of Robotics Research, V4, N2, 1985.
 - 25) Vidyasagar, M., "Non-linear Systems Analysis", Prentice-Hall
 - 26) Vidyasagar, M., Desoer, C. A., " Feedback Systems: Input-Output Properties", Academic Press.
 - 27) Vidyasagar, M., Spong, M. W., "Robust Non-linear Control of Robot Manipulators", IEEE Conference on Decision and Control", December 1985.
 - 28) Whitney, D. E., "Force-Feedback Control of Manipulator Fine Motions", ASME Journal of Dynamic Systems, Measurement, and Control :91-97, June, 1977.
 - 29) Whitney, D. E., "The Mathematics of Coordinated Control of Prosthetic Arms and Manipulators", ASME Journal of Dynamic Systems, Measurement, and Control 94-G(4):303-309, December, 1972.
 - 30) Whitney, D. E., "Quasi-static Assembly of Compliantly Supported Rigid Parts", ASME Journal of Dynamic Systems, Measurement, and Control (104):65-77, March, 1982.
 - 31) Wu, C., Paul, R. P. C., "Manipulator Compliance Based on Joint Torque Control", In Proceedings of the Conference on Decision and Control, pages 88-94. IEEE, Albuquerque, New Mexico, December, 1980.